THEORETICAL AND EXPERIMENTAL STUDY OF THERMAL CONDUCTANCE OF WAVY SURFACES

NASA Research Grant: No. NGR-22-009-065 M.I.T.

Semi-Annual Status Report

Period Covered: November 1964 to June 1965

Prepared by: M. Michael Yovanovich

Submitted by: Professors W. M. Rohsenow and H. Fenech

Table of Contents

Nomenclature

Symbols	Description	Unit
a	radius of heat channel	in.
b	half width of the contour area	in.
c	radius of contact spot	in.
h	contact conductance	BTU/HR-FT^2
k	thermal conductivity	BTU/HR-FT-^{o}F
k_1	material constant	1/psi
l	length in direction of no waviness	in.
n	contact spots	no/in.^{2}
p	apparent pressure	psi.
A	total area	in.^{2}
C	Compliance	in.
E	Modulus of Elasticity	psi.
H	Microhardness	psi.
L	Wave pitch	in.
N	Total number of contact spots	no.
P	Total Load	lb.
R	Contact resestance	^{o}F/BTU/HR
W	Load per unit length of contour contact	lb/in.

Subscripts

1	Surface 1
2	Surface 2
a	Apparent

c	Contour
r	Real
r	Roughness Component
w	Waviness Component

Greek Symbols

ε_1^2	Ratio of real to contour area
ε_2^2	Ratio of contour to apparent area
ε_3^2	Ratio of real to apparent area
σ	Root mean square roughness
$\dot{\sigma}$	Root mean square slope

Introduction

Contact Area of Wavy and Rough Surfaces

Heat transfer in a vacuum takes place through the area of real contact between two surfaces. It is therefore most urgent to obtain a means of determining the real area of contact. Until recently only the contact area between elastically deformed bodies having a curvilinear shape has been considered. But these formulae do not take into account the surface roughness which strongly influences the real area of contact.

Bowden and Tabor (1) in their investigations on the real area of contact proposed the following simple formula

$$A_r = \frac{p}{H}$$

where p is the apparent pressure, H the microhardness. This gives the value of the real area of contact for conditions of full plasticity without considering the roughness or the waviness. The same equation has been used by Holm (2) for the determination of electrical contacts.

Archand (3) in his work determined the real contact area by assuming the asperities to be spherical and that the deformation was purely elastic.

The work done by Dyson and Hirst (4) led to the conclusion that elastic deformation of the surface layer plays an important role in the determination of the real contact area.

We have assumed that the real area of contact can be determined

by the assumption that the deformation of the asperities is plastic and elastic while the waviness deforms elastically. The waviness can be spherical, cylindrical or of no periodic character.

The real surface of a solid body is both rough and wavy. The roughness of a surface is due to irregularities in the surface which result from the inherent action of the production process. These are deemed to include traverse feed marks and the irregularities within them. Roughness can range from 5×10^{-6} inches for very smooth surfaces to $.4000 \times 10^{-6}$ inches for the very rough surfaces.

Waviness is that component of the surface upon which roughness is superimposed. Waviness may result from such factors as machine or work deflections, vibrations, chatter, heat treatment or warping strains. The length of these waves, depending on quite a number of conditions, varies from .04 to 1600×10^{-6} inches.

Each pattern is characterized by the principal direction (or lay) of the predominant surface pattern, by the separation or spacing or its principal crests, by its height normal to the surface (which is generally expressed as a root mean square of its height) and by the shape of the irregularities seen in cross section.

Theoretical Work

The description of the contact area can be reduced to the following types:

1) Apparent or geometrical area of contact A_a which is determined by the overall dimensions of the contacting bodies.

2) Contour area of contact A_c which is the area formed by the bulk compression of the waves. The contour area depends upon the compressing load.

3) Real area of contact A_r which is the sum of the small actual areas of contact. The real area is a function of the loading.

In some cases the area of contact is more conveniently expressed through dimensionless values, e.g.

$$\varepsilon_1^2 = \frac{A_r}{A_c} \tag{1}$$

for the relative area of contact with roughness but without waviness, since $A_c = A_a$,

$$\varepsilon_2^2 = \frac{A_c}{A_a} \tag{2}$$

for the relative area of contact with waviness but without roughness, and

$$\varepsilon_3^2 = \frac{A_r}{A_a} \tag{3}$$

for the relative area of contact with both roughness and waviness. It can be seen that

$$\varepsilon_3^2 = \varepsilon_1^2 \cdot \varepsilon_2^2 \tag{4}$$

When two surfaces are brought together, they will touch in at least three points. As the load is increased, separate contacting irregularities are brought together; through them the applied load is communicated to the wavy region causing compression of these waves.

Under the influence of the applied load the two surfaces approach each other (the compliance increases due to loading) and more asperities come into contact. At the same time, the area of the wave deformation is extended. The waves, in which the strain is always considerably lower than in the peaks, are deformed elastically while part (only those pressed to a high degree) are deformed plastically.

When the load is removed, the elastically deformed region will recover and break both the elastic and plastic microareas of contact. However, part of the plastically deformed asperities will remain in contact.

When waviness is present, the real area of contact is sharply decreased relative to surfaces which are only rough. The growth of the real area of contact is a function of the height of the asperities, their geometrical form and their mechanical properties, of which the most important are the elastic modulus, the yield point and the characteristics of material work-hardening.

As has been shown by experiments, the growth of the number of contacting spots is much greater than the area growth of one spot. For conditions of elastic deformation when cylindrical waviness is available, the area of contact of one spot is slightly dependent upon the load. This can be shown in the following way.

The roughness or contact spots are assumed to be spherical while the waviness or contour spots are cylindrical.

From elastic theory (6), the area of contact can be determined by

$$A_c = c_1 W^{1/2} R^{1/2} l \tag{5}$$

where W is the load per unit length of contact. R is the radius of curvature and l is the surface length in the direction of no waviness. If the contact spots are distributed uniformly over the contour area, i.e. the number of contact spots per unit contour area is n_c, correspondingly, the load per one spot will be

$$W_1 = \frac{W\,l}{A_c n_c} = \frac{W\,l}{c_1 W^{1/2} R^{1/2} l\, n_c} = \frac{W}{c_1 R^{1/2} n_c} \tag{6}$$

The area of one contact spot from elastic theory (6) will be

$$\Delta A_r = c_2\, r^{2/3} W_1^{2/3} = \frac{c_2\, r^{2/3}}{c_1^{2/3} R^{1/3} n_c^{2/3}}\, W^{1/3} \tag{7}$$

The area of contact of one spot is therefore slightly dependent on the load and greatly dependent upon the number of contact spots. We therefore assume that the growth of the contact area is mainly due to the increase in the number of asperities and neglect changes in the radius of the contact spot.

If a sufficiently small region of the surface is considered or if the radius of curvature of the waviness is sufficiently large, then the roughness can be determined by the methods proposed by Fenech and Henry (5).

The relative contact area is independent of the surface size and

therefore the real contact in one contour having the area A_c is equal to $\varepsilon_1^2 \cdot A_c$. Correspondingly, the total area of contact A_r will be equal to the real contact area in one profile multiplied by the number of contours N_c found in the apparent area.

It is obvious that for cylindrical waviness

$$N_c = \frac{A_a}{L\,l} \tag{8}$$

where L is the wave pitch and l is the surface size in the direction of no waviness. The real area of contact can be written

$$A_r = \varepsilon_1^2 \cdot A_c \frac{A_a}{L\,l} \tag{9}$$

If one considers that

$$\varepsilon_3^2 = \frac{A_r}{A_a} \ , \tag{10}$$

then

$$\varepsilon_3^2 = \varepsilon_1^2 \frac{2b}{L} \tag{11}$$

When cylinders with parallel axes are brought in contact, the surface of contact is a narrow rectangle. The investigation (6) of local deformation gives for the half width the expression

$$b = \sqrt{\frac{4\,W\,(k_1 + k_2)\,R_1\,R_2}{R_1 + R_2}} \tag{12}$$

in which R_1 and R_2 are the radii of the cylinders, W is the load per unit length of the surface of contact and k_1 and k_2 are constants defined by

$$k_1 = \frac{1 - \nu_1^2}{\pi E_1} \qquad k_2 = \frac{1 - \nu_2^2}{\pi E_2} \tag{13,14}$$

If both cylinders are of the same material and $\nu = 0.30$, then

$$b = 1.52\sqrt{\frac{W R_1 R_2}{E (R_1 + R_2)}} \tag{15}$$

For the case of two equal radii, $R_1 = R_2 = R$,

$$b = 1.09\sqrt{\frac{W R}{E}} \tag{16}$$

The contour area of contact for identical wavy surfaces can be expressed as

$$A_c = N_c \, 2 \, b \, l \tag{17}$$

where N_c is the total number of waves and l the surface length in the direction of no waviness.

The apparent area of contact can be expressed as

$$A_a = N_c \, L \, l \tag{18}$$

where L is the distance between waves. The real area of contact can be written as

$$A_r = n \, A_c \, \pi \, c^2 \tag{19}$$

where n is the number of contact spots per unit area as determined by graphical means or by statistical methods if the asperities are randomly distributed over the surface.

$$\xi_1^2 = \frac{A_r}{A_c} = n \pi c^2 \tag{20}$$

$$\xi_2^2 = \frac{A_c}{A_a} = \frac{N_c \, 2 \, b \, l}{N_c \, L \, l} = \frac{2 \, b}{L} \tag{21}$$

$$\varepsilon_3^2 = \frac{A_r}{A_a} = \frac{A_r}{A_c} \cdot \frac{A_c}{A_a} = \varepsilon_1^2 \cdot \varepsilon_2^2 \qquad (22)$$

By assuming that the roughness is deformed plastically the following relationship is found

$$\frac{A_r}{A_c} = \varepsilon_1^2 = \frac{P}{H} \qquad (23)$$

Roughness Coefficient of Heat Transfer in the Presence of Waviness

The solution for the constriction resistance of an isothermal circular area of radius c on the surface of a semi-infinite body of width a, i.e. $c \ll a$ was given by Holm (2) as

$$R = \frac{1}{4 \cdot c \cdot k} \qquad (24)$$

where k is the thermal conductivity of the material. For two semi-infinite bodies having the same material properties, the contact resistance becomes

$$R = \frac{1}{2 \cdot c \, k} \qquad (25)$$

If both members were identical and had equal constrictions, then the contact area would be isothermal due to symmetry.

The total resistance for N contact spots can be approximated by

$$R = \frac{1}{2 N c k} \left(1 - 1.04 \frac{c}{a} \right) \qquad (26)$$

The conductance can be expressed as

$$\frac{1}{h_r} = \frac{1 - 1.64 \, \varepsilon_1}{2 \frac{\sqrt{n}}{\sqrt{\pi}} \varepsilon_1 \, k} \qquad (27)$$

Waviness Coefficient of Heat Transfer

According to Holm the resistance for an elliptic contact can be expressed by determining the resistance for a circular contact and then modifying the results by a form factor.

$$R\ (c,\ c) = R\ (b,\ 1)\ f\ (b/1) \tag{28}$$

$$\therefore\ h_w = \frac{2}{L\ 1}\ \frac{k}{f\ (b/1)} \tag{29}$$

Total conductance for wavy and rough surfaces in a vacuum environment can be written as

$$\frac{1}{h} = \frac{1 - 1.64\,\varepsilon_1}{\frac{2}{\sqrt{\pi}}\sqrt{n'}\varepsilon_1 k} + \frac{1}{\varepsilon_2 k\sqrt{\frac{2}{L\ 1}}\ \frac{1}{f\ (b/1)}} \tag{30}$$

Experimental Determination of Contact Conductance

Description of Apparatus

The experimental apparatus is shown in figure 1 and consists of a structure for support and loading, the test chamber, a vacuum system and an instrument console.

The physical load is obtained by means of the lever system which provides dead weight loading to the test section. Dead weight loading is independent of thermal strains resulting when the test section is heated. The actual load on the test specimens is measured directly by a strain gauge dynamometer.

When the tests are run in a vacuum, the minimum load is 103 pounds (or 131 psi in the one-inch diameter test section) due to the atmospheric pressure acting across the 3-inch diameter bellows through which the loading system is attached to the vacuum chamber.

An assembly drawing of the test section and chamber is shown in figure 2. The chamber is a vacuum enclosure consisting of a top plate and upper cylinder, a baseplate which is bolted to the support structure and to which is attached the vacuum system, and a lower flanged cylinder bolted to the upper cylinder and baseplate.

The test section (see figure 2) consists of, from top to bottom: the upper cooler (part 4), spacers (5 and 6) of materials chosen to have conductivities appropriate for the test being conducted, the upper heater (7), the upper heat meter (8), the two test specimens (9, 10) the lower heat meter (15), the lower heater (16) and insulating spacer (17), the dynamometer (18), and the

lower cooler (19).

Some flow of water is maintained in all coolers during testing in order to protect the top and base plates. The heating elements are Kanthal resistance wire coiled and cemented between an alundum core and outer sleeve. The heater cores are one-inch diameter stainless steel.

All thermocouples are 28-gauge chromel-alumel cemented into place using Sauereisen. Four thermocouples are inserted into each test specimen spaced along the center line.

The dynamometer is a 1-1/2 inch diameter 2-inch long aluminum cylinder located between the lower cooler and lower insulation. Near the base of the cylinder semi-conductor steam gauges are attached. The basic sensitivity of the dynamometer is about 1 millimeter displacement on the Sanborn recorder readout for a one-pound load.

In order to minimize radiation losses from the test section, a radiation shield is provided as shown in figure 2.

The vacuum system consists of a mechanical forepump, a 4-inch diffusion pump with a water-cooled optical baffle, and a three-way vacuum valve. Pressures between 5 and 1000 microns of Hg are read with a thermocouple gauge, and the range between 5 microns and 10^{-7} mm. Hg is read with an ionization gauge.

The instrument console is shown in figure 3. Power for the four heaters and the pumps is controlled from the console. The thermocouple potentiometer, wattmeters for the heaters, and the vacuum gauge control are located on the console as are valves for controlling

the flows through the four coolers.

Experimental Procedure

The apparatus described above was used to obtain data for stainless steel contacts in a vacuum environment. The samples were positioned and the test section was aligned under a load of about 20 psi. After having aligned the specimens, the chamber was closed and a vacuum of about 5×10^{-6} mm Hg was attained. With a minimum interface pressure of 131 psi., all heaters were turned on producing an interface temperature of about 700° F. The system and interface were allowed to outgas for about 36 hours after which there was no noticeable change with time of the contact conductance.

The outgassing of the interface having been completed, the load was increased in increments, temperature readings were taken. About four hours were required to achieve thermal equilibrium in the test section subsequent to increasing the load.

The first pair of specimens were stainless steel having roughness but no waviness. The second pair of specimens were stainless steel having waviness but no roughness.

Stainless Steel Surfaces in a Vacuum

The first pair of surfaces were prepared from 1-1/2 inch long, 1-inch diameter type 416 stainless steel cylinders. These cylinders were ground and lapped to produce a flat surface with a roughness number of 3. The surfaces were tested and no waviness was found to be present. The surfaces were then blasted with glass spheres to achieve roughness of about 100×10^{-6} inches. The resulting surfaces

were judged to have non-directional properties so that any of their profiles may be considered to be representative of the surface.

The thermal conductivity of the stainless steel was determined by comparison of the temperature gradient in stainless steel and armco-iron. Over a temperature range of 200 - 600 ^{o}F the conductivity was found to be constant at 14.6 Btu/hr/ft ^{o} F.

Profiles of the surfaces were obtained. The height of the profile was read for 1000 equally spaced points, and the auto correlation function for each profile and its second derivative at zero were determined by the digital computer. The surface properties were determined to be:

$$\sigma_1 = 131 \times 10^{-6} \text{ inches} \qquad \dot{\sigma}_1 = .107$$

$$\sigma_2 = 103 \times 10^{-6} \text{ inches} \qquad \dot{\sigma}_2 = .097$$

The number of contact spots per unit area were determined graphically and is shown in figure 4 as $\sqrt{n}$ versus compliance.

The ratio of actual area to apparent area is shown plotted in figure 5 as ε vs compliance and was determined graphically from the profiles.

In figure 6 is shown the apparent pressure versus compliance for stainless steel. This curve was also obtained by graphical means and assuming that the asperities were deformed plastically.

Using these data from figures 4 through 6, the contact conductance was calculated according to equation (27). The theoretical values and the test data are plotted in figure 7. The theoretical values and the loading test data are seen to agree fairly well at

the lower loads but deviate considerably at the higher loads. The unloading test data is seen to disagree with theory at the low loads due to the permanent plastic deformation of the highest asperities.

The second pair of specimens tested were prepared with a wavy surface having radius of curvature of 1/16 inch and a pitch of 1/4 inch. The surfaces were not rough.

An examination of figure 9 shows very clearly that the deformation of the asperities is not completely elastic nor completely plastic over the entire load range as assumed by Clausing (8) and Fenech (9) respectively. The test values indicate that the first asperities initially deform plastically, then as the number of asperities coming into contact increases very quickly, the deformation tends towards the elastic curve. Finally as the load becomes very large, all the asperities begin to deform plastically with still some elastic effect. Over the entire load range the test data fell between the two limiting curves for completely elastic and completely plastic deformation.

Current Status

At present wavy surfaces having a roughness are being prepared on the four materials stainless steel, aluminum, magnesium, and brass.

The wavy component will be cylindrical in shape, having a pitch of 1/4 inch and a height of about 1000×10^{-6} inches. The roughness will be of the order of 150×10^{-6} inches.

These surfaces will be tested as described under experimental procedure and compared with the theory.

Some analytical work will have to be done to better correlate the compliance versus the applied pressure. Curves will be produced for completely elastic deformation and for completely plastic deformation. The test data is expected to fall between these two limits and a correction will accordingly be applied to the analytical work.

Proposed Future Work

It is proposed to try to explain analytically or to correlate the elastic and plastic deformation of rough flat surfaces.

Curves such as figure 9 for Stainless Steel will be prepared for Aluminum and Magnesium. Test data will also be obtained to permit the correlation of the conductance versus load with proper consideration of the elastic-plastic deformation of the surface.

References

1. Bowden, F. P. and Tabor D., "Friction and Lubrication of Solids," Oxford University Press, 1950.
2. Holm, R., "Electric Contacts Handbook," Springer-Verlag Berlin/Gottingen/Heidelberg, 1958.
3. Archand, J. F., "Elastic Deformation and the Laws of Friction," Proc. Roy. Soc. (London), A, 243 (1957) 190.
4. Dyson, J. and Hirst, W., Proc. Roy. Soc. (London), B, 67 (1954) 309.
5. Henry, J. J. and Fenech, H., "The Use of Analog Computers for Determining Surface Parameters Required for Prediction of Thermal Contact Conductance," ASME Paper No. 63-WA-104.
6. Timoshenko, S. and Goodier, J. N., "Theory of Elasticity," McGraw-Hill, New York, 1951.
7. Hoffman, O. and Sachs, G., "Introduction to the Theory of Plasticity for Engineers," McGraw-Hill, New York, 1953.
8. Clausing, A. M. and Chao, B. T., "Thermal Contact Resistance in a Vacuum Environment," NASA, University of Illinois, ME-TN-242-1, August, 1963.
9. Fenech, H., and Rohsenow, W. M., "Thermal Conductance of Metallic Surfaces in Contact," U.S. Atomic Energy Commission Report NYO-2136, May, 1959.

List of Figures

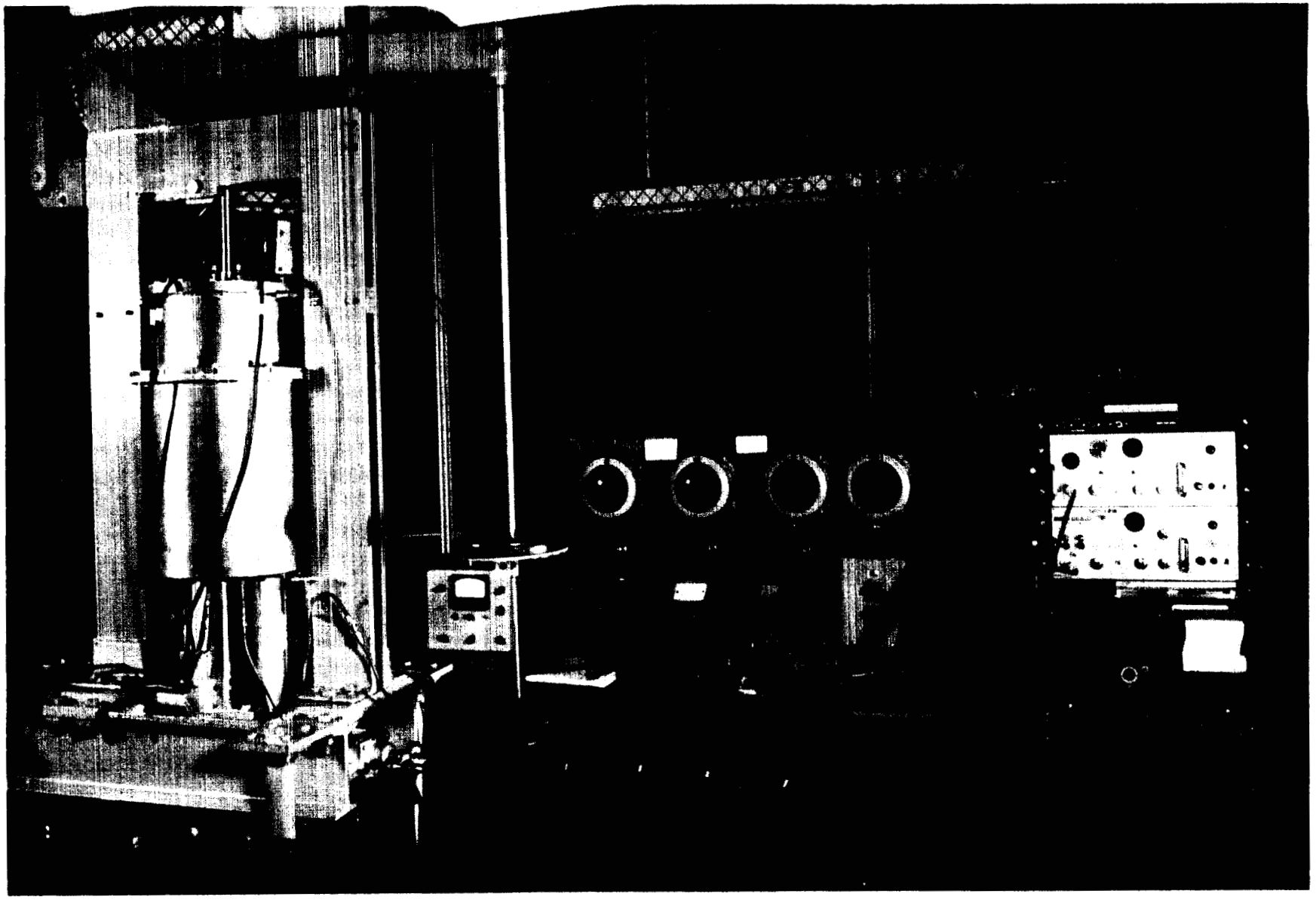

FIGURE 1. EXPERIMENTAL APPARATUS

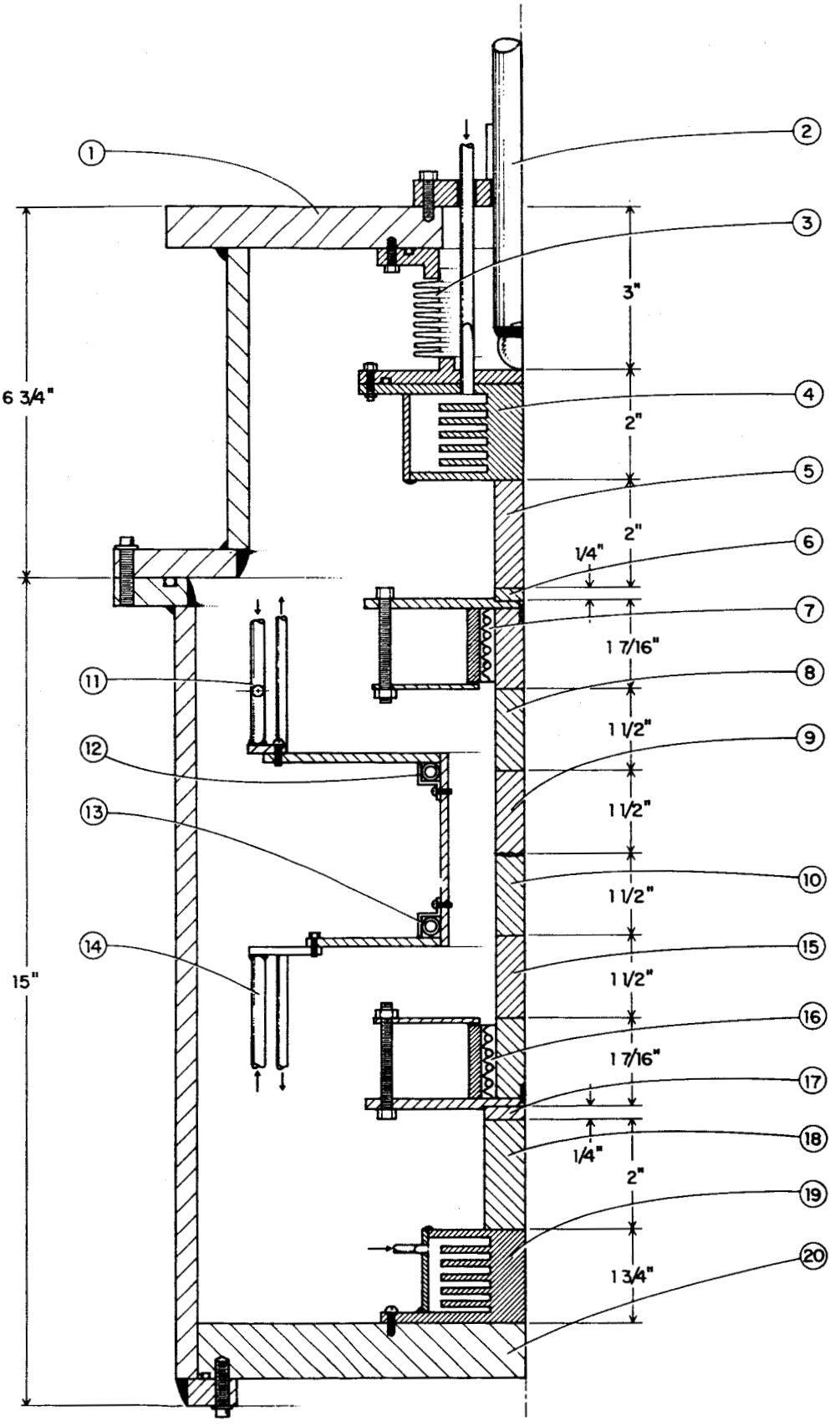

FIGURE 2. SECTION THROUGH TEST SECTION AND CHAMBER

PARTS LIST FOR FIGURE 16

Part No.	Description
1	Top Plate
2	Loading Mechanism
3	Bellows
4	Upper Main Cooler
5	Spacer of Optional Conductivity
6	Transite Spacer
7	Upper Main Heater
8	Upper Heat Meter
9	Upper Sample
10	Lower Sample
11	Guard Ring: Upper Guard Ring Cooler
12	Upper Guard Ring Heater
13	Lower Guard Ring Heater
14	Lower Guard Ring Cooler
15	Lower Heat Meter
16	Lower Main Heater
17	Transite Spacer
18	Dynamometer - Aluminum Cylinder
19	Lower Main Cooler
20	Base Plate

Top Plate Mountings (Not Shown on Figure 16)

1	Adjustable Vacuum Leak
2	Upper Main Heater Power Feedthrough (2 Terminals)

Top Plate Mountings (Not Shown on Figure 16) (Continued)

3	Upper Guard Ring Heater Power Feedthrough (2 Terminals)
4	Upper Main Cooler Feedthrough (Inlet and Outlet)
5	Upper Guard Ring Cooler Feedthrough (Inlet and Outlet)
6	Thermocouple Feedthroughs (2 with 8 Thermocouples Each)

Base Plate Mountings (Not Shown on Figure 16)

1	Lower Main Heater Power Feedthrough (2 Terminals)
2	Lower Guard Ring Heater Power Feedthrough (2 Terminals)
3	Lower Main Cooler Feedthrough (Inlet and Outlet)
4	Lower Guard Ring Cooler Feedthrough (Inlet and Outlet)
5	Thermocouple Feedthrough (For Up to 8 Thermocouples)
6	Dynamometer Signal Feedthrough

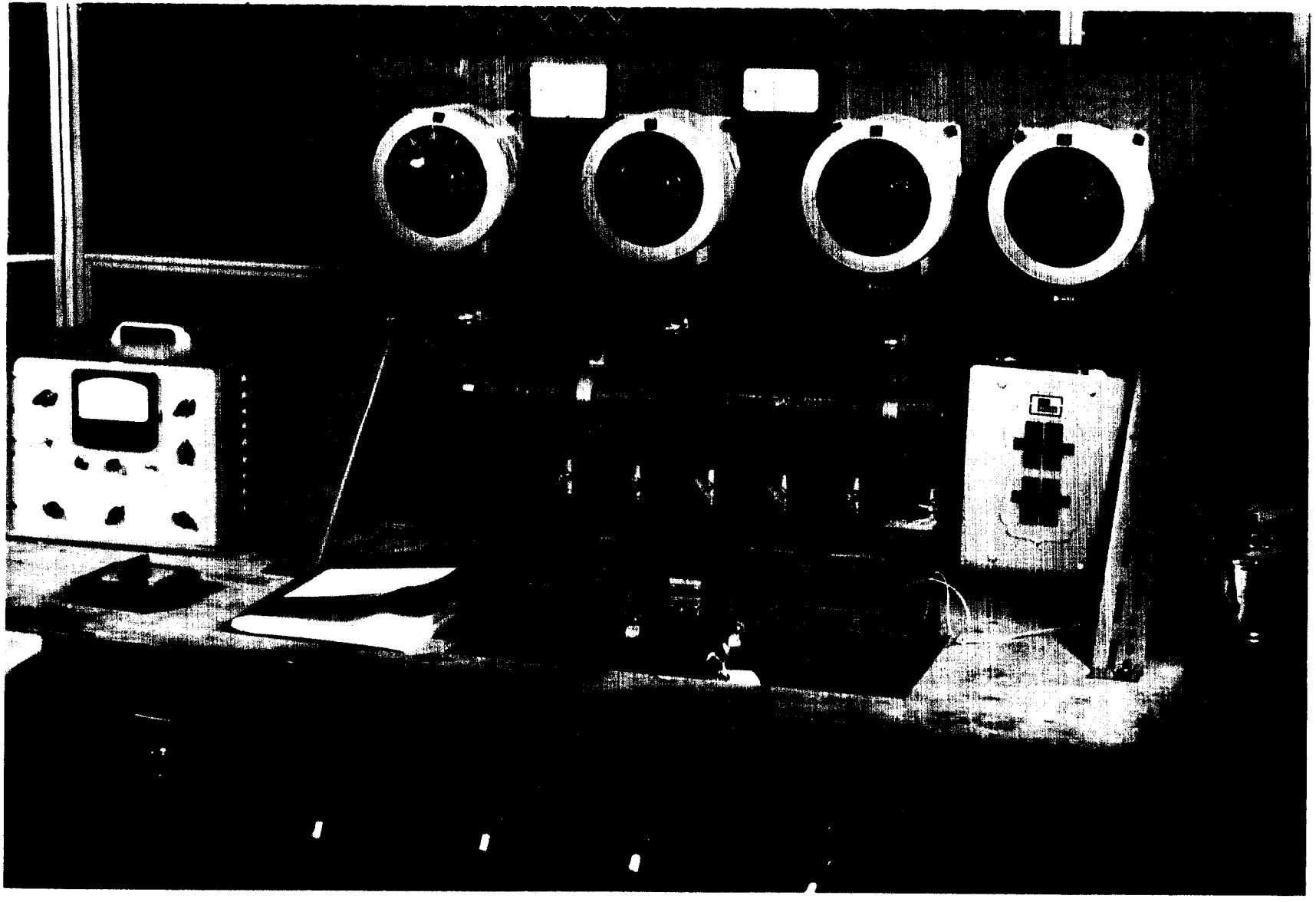

FIGURE 3. INSTRUMENT CONSOLE

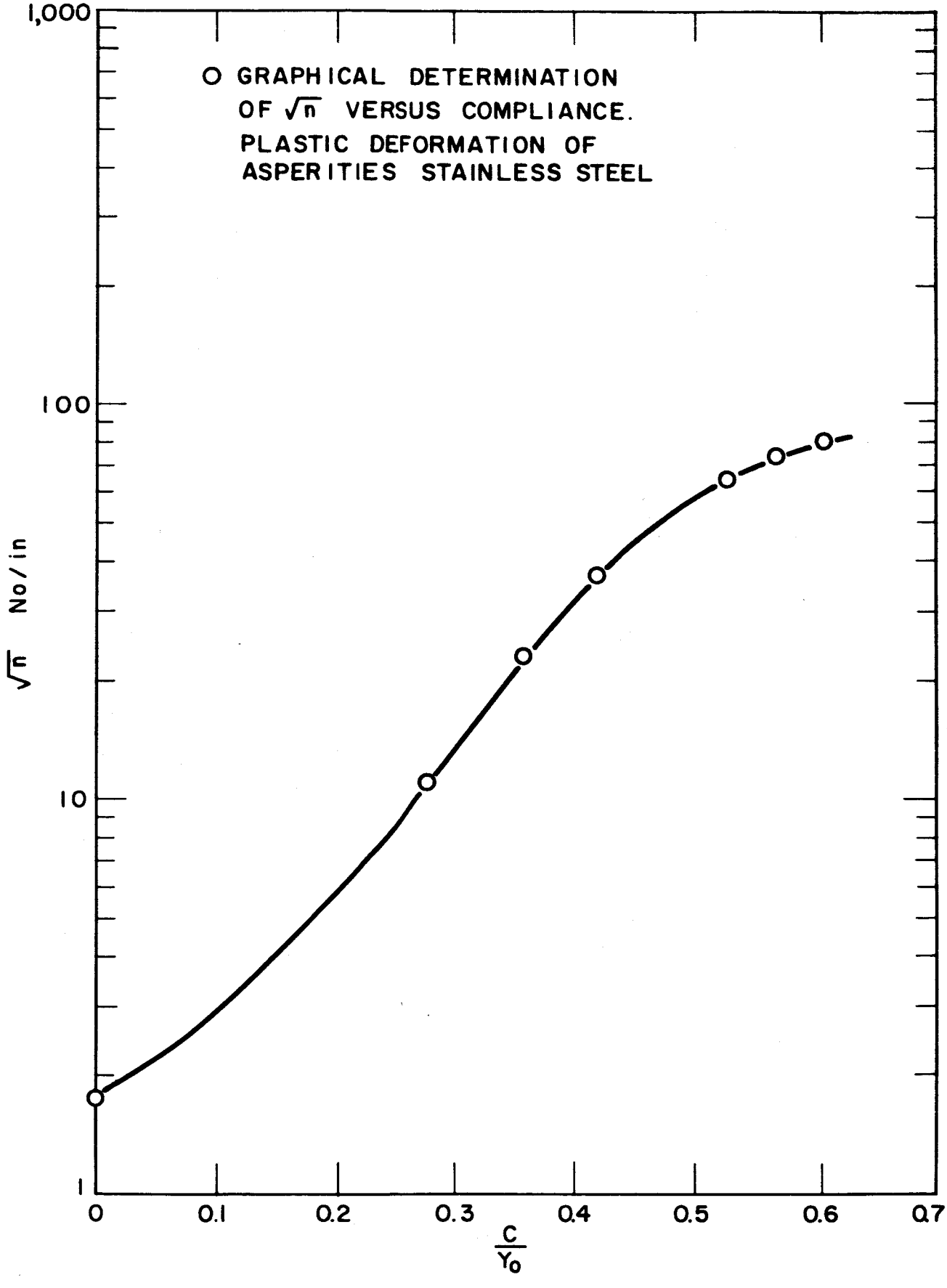

FIGURE 4. NUMBER OF CONTACT SPOTS VERSUS COMPLIANCE

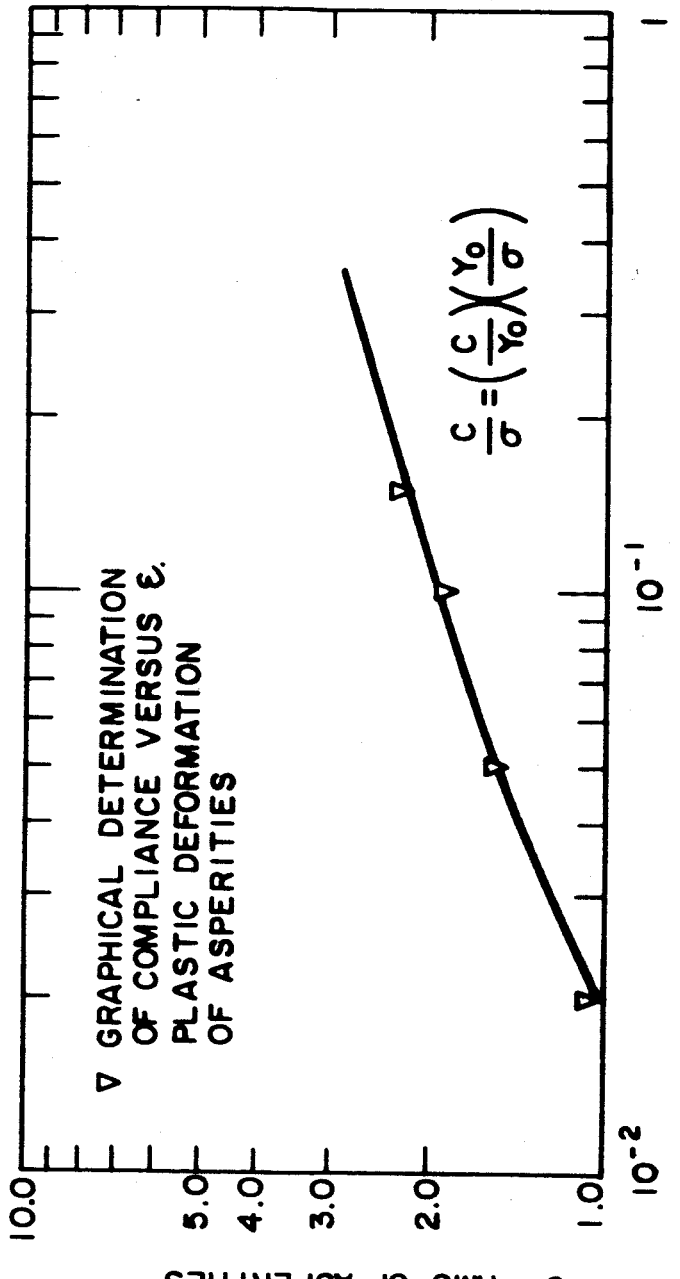

FIGURE 5. COMPLIANCE VERSUS ε FOR STAINLESS STEEL

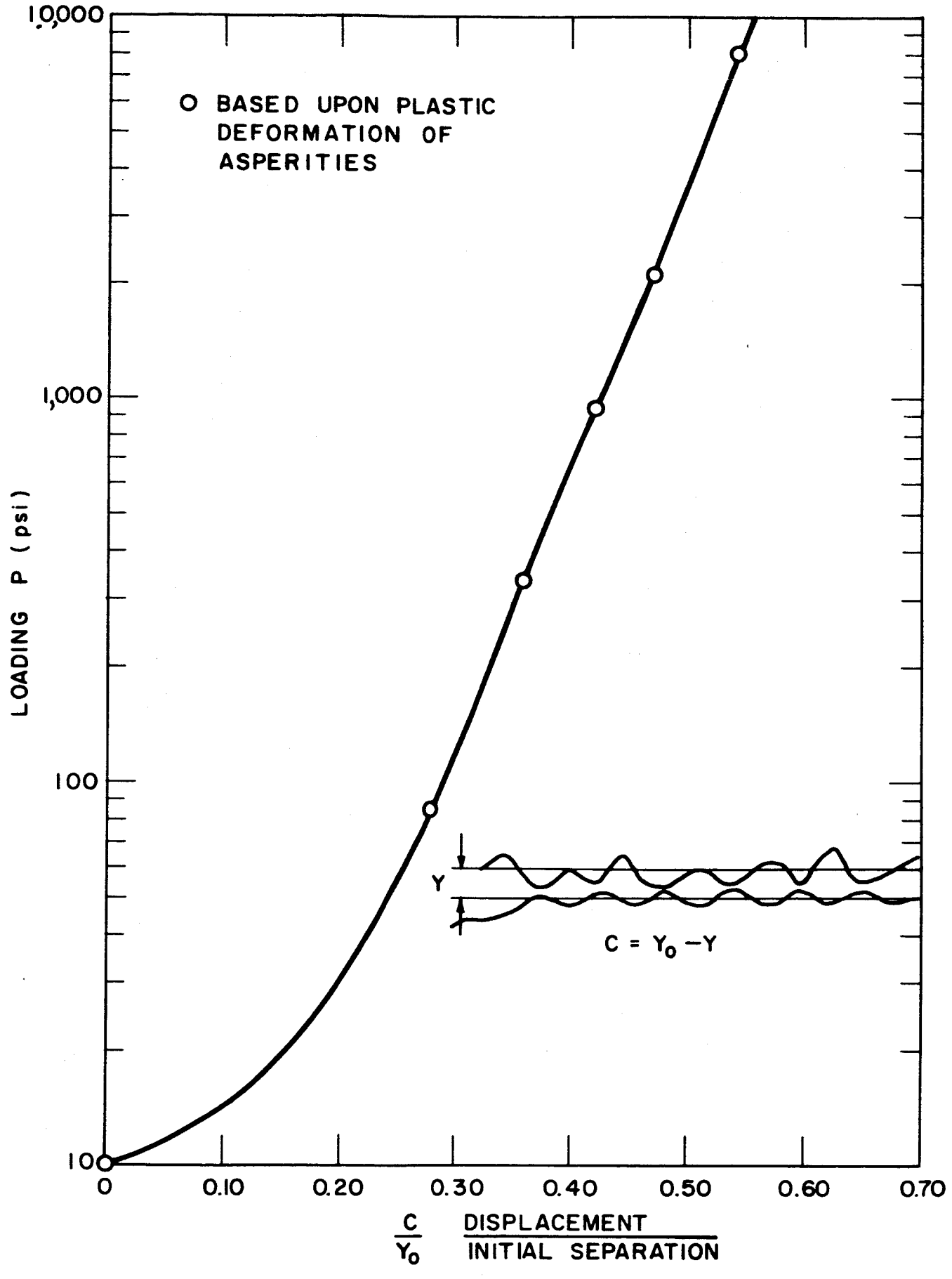

FIGURE 6. LOADING VERSUS COMPLIANCE FOR STAINLESS STEEL

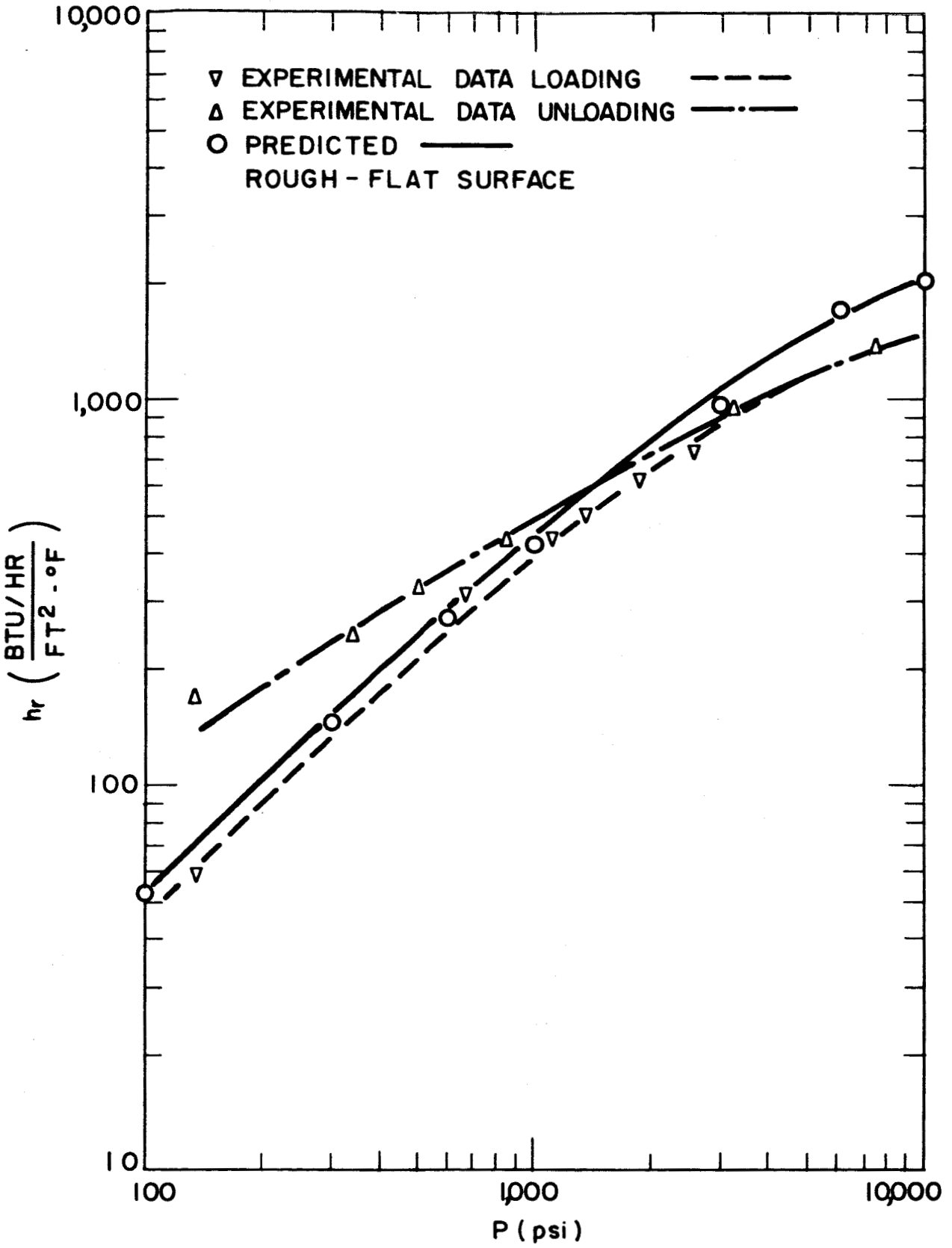

FIGURE 7. RESULTS FOR STAINLESS STEEL IN A VACUUM

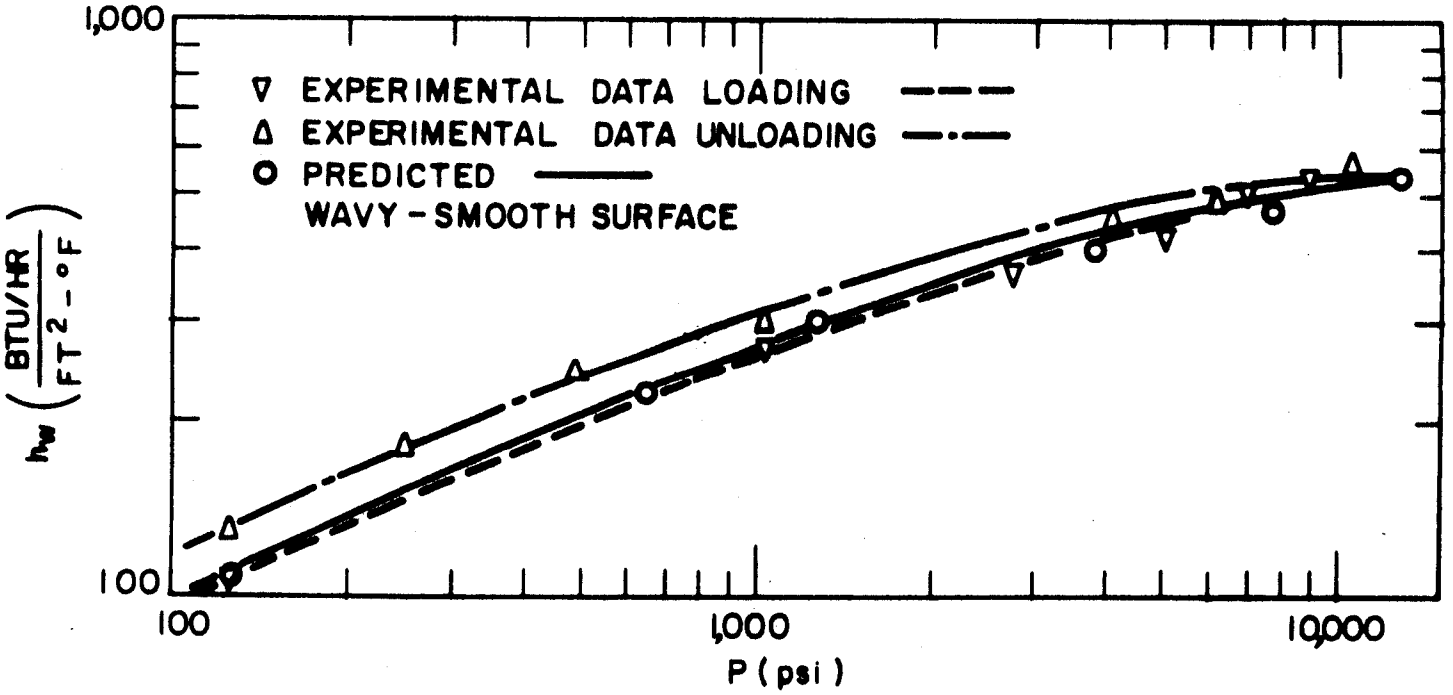

FIGURE 8. RESULTS FOR STAINLESS STEEL CONTACT IN A VACUUM

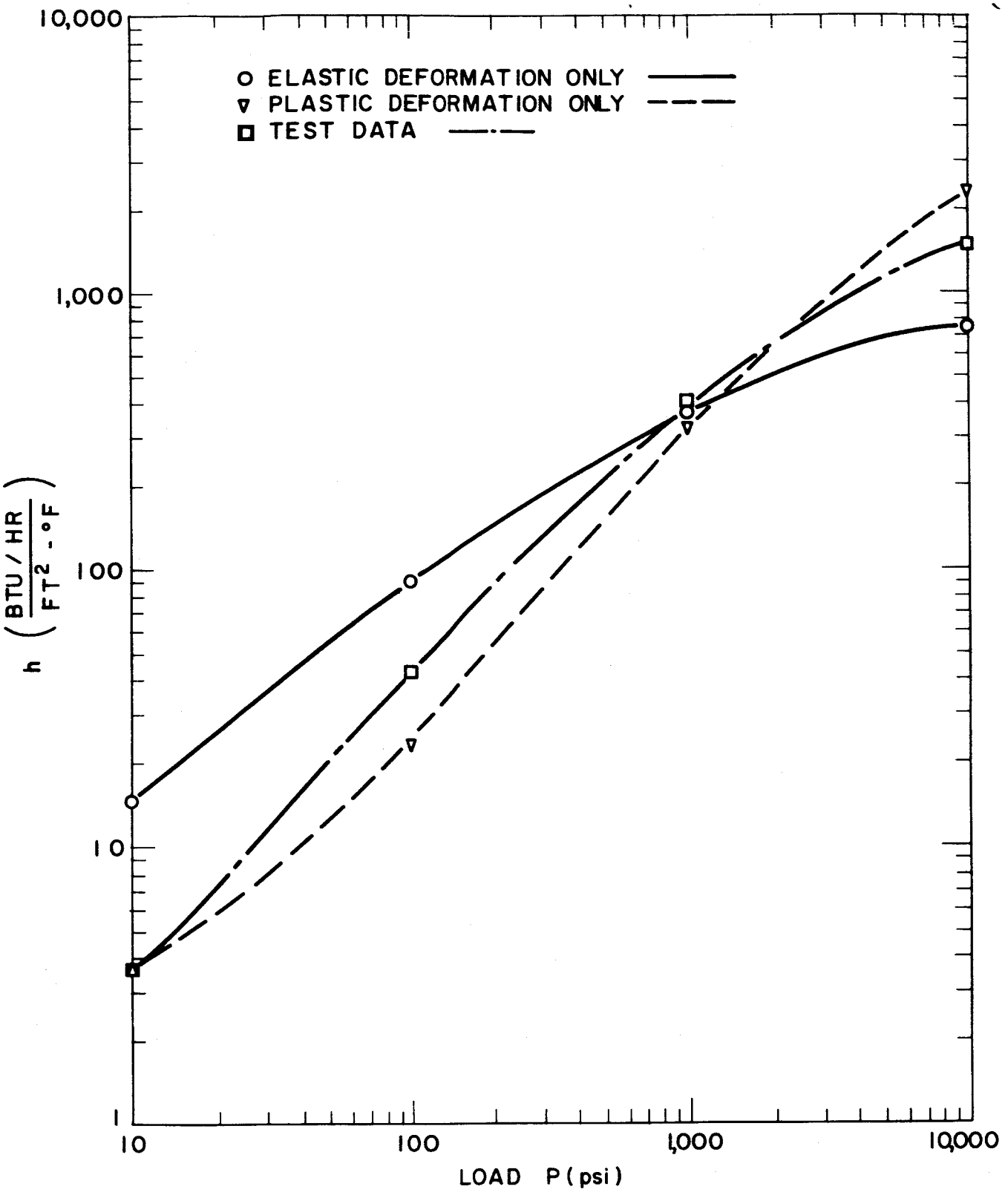

FIGURE 9. THERMAL CONTACT CONDUCTANCE VERSUS LOAD FOR STAINLESS STEEL